Research Article

Rajendran Selvamani*, Rubine Loganathan, Rossana Dimitri, and Francesco Tornabene

Nonlocal state-space strain gradient wave propagation of magneto thermo piezoelectric functionally graded nanobeam

https://doi.org/10.1515/cls-2022-0192
received November 17, 2022; accepted March 12, 2023

Abstract: In this work, the state -space nonlocal strain gradient theory is used for the vibration analysis of magneto thermo piezoelectric functionally graded material (FGM) nanobeam. An analysis of FGM constituent properties is stated by using the power law relations. The refined higher order beam theory and Hamilton's principle have been used to obtain the motion equations. Besides, the governing equations of the magneto thermo piezoelectric nanobeam are extracted by developed nonlocal state-space theory. And to solve the wave propagation problems, the analytical wave dispersion method is used. The effect of magnetic potential, temperature gradient, and electric voltage in variant parameters are presented in graph.

Keywords: wave propagation, functionally graded materials, nonlocal strain gradient state-space theory, magneto piezoelectric nanobeam

1 Introduction

Functionally graded materials (FGMs) are a type of composites initiated by a group of Japanese scientists to control the volume fraction of the mixture of two or more materials. The nonlinear vibration of the piezoelectric nanobeams based on the nonlocal and Timoshenko theory, the influence of the nonlocal parameter, temperature change, and external electric voltage on the size dependent nonlinear vibration characteristics of the piezo electric nanobeam are exposed [1]. Researchers [2] studied the natural frequencies along with mechanical and thermo electric vibration of piezoelectric nanobeams based on the nonlocal theory. Ebrahimi [3] reported the scattering of waves of FG nanobeam of viscoelastic nature. In the framework of third-order shear deformation theory [4], the vibration characteristics of functionally graded (METE-FG) nanobeams were analyzed. And the free vibrations of FG nano plates resting on elastic foundation *via* Hamilton principle was dealt in detail [5]. Alibeigi *et al.* [6] introduced the buckling retaliation of nanobeams on the basis of the Euler–Bernoulli beam model with the von Kármán geometrical nonlinearity. Bending of flexo electric magneto-electro-elastic (MEE) nanobeams lying over Winkler–Pasternak according to nonlocal elasticity theory has been studied [7]. Several studies were conducted on [8–10] hygro-thermal loading, the bending analysis of magneto-electro piezoelectric nanobeams system, dynamic analysis of smart nanostructures, and frequency analysis of thermally post buckled FGM thin beams. Stress-driven *vs* strain-driven elastic nanobeams have been discussed *via* integral elasticity [11,12]. Using the kinematic model, Kiani and Eslami [13] reported the buckling of beams made of FG under different types of thermal loading. The propagation of wave of infinite functionally graded plate in thermal environment was reported by Sun and Luo [14]. A consistent refined HSDT is designed to probe the free vibration of GF plates on elastic foundation and the influence of boundary condition on the natural frequency [15]. The different working conditions of the nano sized elements were studied by Thai *et al.* [16]. By considering the nonlocal elasticity [17], a prediction has been made that the essential behaviors of the nanostructures cannot be same as the macro scale structures. The Euler–Bernoulli beam theory was used to study the bending analysis of microtubules (MT) by Eringen [18]. Based on Euler–Bernoulli beam theory, the bending analysis of MT

* **Corresponding author: Rajendran Selvamani,** Department of Mathematics, Karunya Institute of Technology and Sciences, Coimbatore, 641114, Tamilnadu, India,
e-mail: selvamani@karunya.edu
Rubine Loganathan: Department of Mathematics, Karunya Institute of Technology and Sciences, Coimbatore, 641114, Tamilnadu, India, e-mail: rubineloganathan5@gmail.com
Rossana Dimitri, Francesco Tornabene: Department of Innovation Engineering, University of Salento, Lecce, Italy

was studied using the method of Differential Quadrature (DQ) by Civalek and Demir [19]. Using finite element method (FEM) [20], the nonlinear bending in nanobeams were discussed. Reddy and El-Borgi [21] investigated the dispersion of waves with the effects of surface stresses in smart piezoelectric nanoplates. Bi-directional FGM nanobeams with the characteristics of bending, buckling, and vibrational nonlocal elements were concentrated in some of the previous studies [22–24]. The natural frequency variation located on a viscoelastic sheet was surveyed by using the nonlocal theory [25]. The size-dependent elements of beam were analyzed by Ebrahimi and Barati [26]. Nonlocal elasticity and its running conditions are discussed in details in the literature [27]. Based on the nonlocal strain gradient theory (NSGT) [28], the thermo-mechanical buckling problem of graphene sheets was proposed. Stiffness, softening, and hardening effect of FG beam were studied by Li *et al.* [29]. Solving the wave dispersion problem of nanoplates was accomplished by Ebrahimi and Dabbagh [30] with the application of infusing NSGT and surface-related elasticity for responsive piezoelectric materials. With the small-scale effect, the free vibration of 3D FGM Euler–Bernoulli nanobeam was studied by Hadi *et al.* [31]. Alibeigi *et al.* [32] exposed the buckling response of a nanobeam on the basis of the Euler–Bernoulli beam model using a couple stress theory under various types of thermal loading and an electrical and magnetic field. Timoshenko beam theory was investigated by Ke and Wang [33] with the rise in uniform temperature, magnetic potential, and external electric potential *via* nonlocal form to MEE vibrations. Bending of MEE nanobeam was studied in detail by Ebrahimi *et al.* [34]. Along with that, Ebrahimi *et al.* [35] investigated the bending of MEE nanobeams relating the nonlocal elasticity theory under hygro-thermal loading embedded in Winkler–Pasternak foundation. The size dependent problems using nonlocal elasticity theory, nonlocal couple stress theory, and shear deformation theory were reported [36,37]. Ebrahimi *et al.* [38] discussed the effects of various parameters on the wave dispersion characteristics of size-dependent nanoplates. The thermal effects on the buckling and free vibration of the FG nanobeams is documented well in the literature [39]. Ebrahimi and Barati [40] discussed the damping vibration characteristics of the hygro-thermally affected FG viscoelastic nanobeams. The thermal effect on buckling and free vibration characteristics of size-dependent Timoshenko nanobeams, and the free vibration of curved FG nano size beam in thermal environment been discussed in the literature [41,42]. The buckling and vibration properties of sandwich FG beams were studied by Vo *et al.* [43]. Jalaei *et al.* [44] studied the thermal and magnetic effects on the FG Timoshenko nanobeam. Studies over the hygro-thermal wave characteristic of nanobeam of an inhomogeneous material with porosity under magnetic field is notable [45].

Hence, this work shows the wave propagation analysis of FG nanobeam with the help of a nonlocal state-space strain gradient viscoelasticity. The magneto thermo material properties of the nanobeam also graded and implemented *via* power law relations and the motion equations are deduced through the Hamilton's principle. Furthermore, the dispersion for computed external electric voltage, magnetic effect, and the gradient of temperature are presented with graphical solution.

2 Mathematical formulations

Based on the state-space nonlocal strain gradient theory, the length L, width b, and thickness h of a viscoelastic FG nanobeam has been investigated (Figure 1). The two parts of constituent FGM are composed of ceramic part and metallic part. The components of FGM are considered to be temperature dependent to evolve a realistic viscoelastic study.

In this section, power-law relations have been used to compute the properties. To calculate the temperature variable towards the thickness direction, the volume fraction of each phase must be calculated by using the power-law model. Hence, the volume fraction of ceramic partis given as follows:

$$V_c = \left(\frac{z}{h} + \frac{1}{2}\right)^p, \tag{2.1}$$

where the thickness h and the exponential power law p probe each phase in the material with its distribution of properties. By considering any desired material property at the local temperature

$$P = P_0(P_{-1}T^{-1} + 1 + P_1T + P_2T^2 + P_3T^3), \tag{2.2}$$

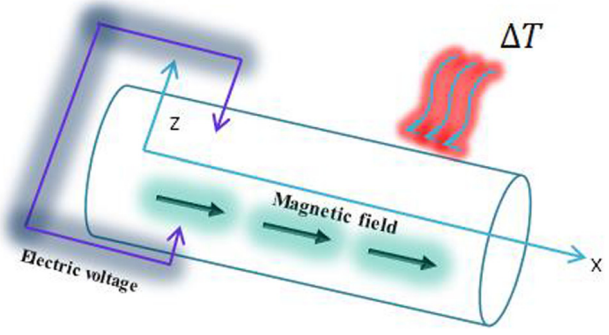

Figure 1: Vibration analysis of FG nanobeam.

where $P_0, P_{-1}, P_1, P_2, P_3$ are the coefficients of material phases. The volume fraction of the metallic phase gives the volume fraction of the ceramic phase by $V_m = 1 - V_c$.

According to Eringen's nonlocal theory, the stress state at a point inside a body is a function of the strains at all points in the neighboring regions. The basic equations with zero body force can be defined as follows:

$$\begin{aligned}\sigma_{ij} &= \int_v \alpha(|y' - y|, \tau)[C_{ijkl}\varepsilon_{kl}(y') - e_{mij}E_m(y') - \Omega_n(y') \\ &\quad - C_{ijkl}\alpha_{kl}\Delta T]\mathrm{d}V(y') \\ D_i &= \int_v \alpha(|y' - y|, \tau)[e_{ikl}\varepsilon_{kl}(y') - E_m(y') + \Omega_n(y') \\ &\quad - \Delta T]\mathrm{d}V(y') \\ B_i &= \int_v \alpha(|y' - y|, \tau)[\varepsilon_{kl}(y') + E_m(x') + \chi_{ni}\Omega_n(y') \\ &\quad - \lambda_i\Delta T]\mathrm{d}V(y'),\end{aligned} \tag{2.3}$$

where σ_{ij}, ε_{ij}, D_i, E_i, respectively, represent the stress, strain, electric displacement, and electric field and B_i, Ω_i are the magnetic induction and magnetic field. α_{kl} and ΔT stand for thermal expansion and temperature difference. C_{ijkl}, e_{mij}, and χ_{ij} are the elastic, piezoelectric, and magnetic constants, respectively, and $\tau = e_0 a/l$ defines the scale coefficient, e_0 is the material constant, and a and l are the characteristic length in the internal and external sides.

The governing equations of the nanobeams are obtained by an accurate kinematic theory. Higher order shear deformation theory also reveals stress-strain changes in solid bodies. From the previous study [8], we can take the refined shear deformable beam's displacement as follows:

$$\begin{aligned}\prod_x(x, z, \tilde{t}) &= \prod(x, \tilde{t}) - \frac{\partial w_b(x, \tilde{t})}{\partial x}z - \frac{\partial w_s(x, \tilde{t})}{\partial x}f(z) \\ \prod_z(x, z, \tilde{t}) &= w_b(x, \tilde{t}) + w_s(x, \tilde{t}),\end{aligned} \tag{2.4}$$

where Π, w_b, and w_s are the longitudinal displacement, bending, and shear components of the transverse displacement. Furthermore, in order to distribute the shear strain, $f^*(z)$ is the shape function which is designed as follows [4]:

$$f^*(z) = \frac{he^z}{h^2 + \pi^2}\left[\pi \sin\left(\frac{\pi z}{h}\right) + h\cos\left(\frac{\pi z}{h}\right)\right] - \frac{h^2}{h^2 + \pi^2}, \tag{2.5}$$

To capture the shear strain and stress, the deformed structural cross section is uncertain with this function. At free surfaces, it is required to satisfy the assumption of shear strain nonexistence. By continuum infinitesimal strain tensor, the nonzero strains can be measured as follows:

$$\begin{aligned}\varepsilon_{xx} &= \frac{\partial \Pi}{\partial x} - z\frac{\partial^2 w_b}{\partial x^2} - f(z)\frac{\partial^2 w_s}{\partial x^2} \\ \gamma_{xz} &= g(z)\frac{\partial w_s}{\partial x},\end{aligned} \tag{2.6}$$

where $g(z) = 1 - \frac{\mathrm{d}f(z)}{\mathrm{d}z}$.

2.1 Motion equations

In accordance with Hamilton's principle, the extended Lagrangian can be given as follows:

$$\dot{L} = \dot{\prod} - \dot{T} + \dot{V}, \tag{2.7}$$

So, the Hamilton's principle can be given as follows:

$$\delta\int_{\tilde{t}_1}^{\tilde{t}_2}\left(\dot{\prod} - \dot{T} + \dot{V}\right)\mathrm{d}\tilde{t} = 0, \tag{2.8}$$

In Eq. (2.8), variables $\prod$, V, and T are the strain energy, work done, and kinetic energy, respectively. Hence, the virtual strain energy can be given as follows:

$$\delta\dot{\prod} = \int_\forall (\sigma_{ij}\delta\varepsilon_{ij}d\forall - D_xE_x - D_zE_z)\mathrm{d}z\mathrm{d}x, \tag{2.9}$$

$$\phi(x, z, \tilde{t}) = -\cos(\beta z)\phi(x, \tilde{t}) + \frac{2zV_0}{h}\mathrm{e}^{-ik\tilde{t}}, \tag{2.10}$$

where $D_x = e_{15}\gamma_{xz} + e_{11}E_x$ and $D_z = e_{31}\varepsilon_{xx} + e_{33}E_z$. The variation in electric potential in the x direction is $\beta = \pi/h; \phi(x, \tilde{t})$; V_0 and Ω are the external electric voltage and natural frequency of the piezoelectric nanobeam, respectively.

By infusing Eq. (2.6) in Eq. (2.9),

$$\begin{aligned}\delta\Pi = \int_0^L\Bigg(&N\frac{\partial\delta\Pi}{\partial x} - M_b\frac{\partial^2\delta w_b}{\partial x^2} - M_s\frac{\partial^2\delta w_s}{\partial x^2} \\ &+ Q\frac{\partial\delta w_s}{\partial x} - D_xE_x - D_zE_z\Bigg)\mathrm{d}z\mathrm{d}x,\end{aligned} \tag{2.11}$$

and the stress resultants can be obtained as follows:

$$[N, M_b, M_s] = \int_A [1, z, f(z)]\sigma_{xx}\mathrm{d}A, \tag{2.12}$$

$$Q = \int_A g(z)\sigma_{xz}\mathrm{d}A, \tag{2.13}$$

The kinetic energy of the system can be determined as follows:

$$\delta T = \int_\forall \rho(z)\left(\frac{\partial\Pi_x}{\partial\tilde{t}}\frac{\partial\delta\Pi_x}{\partial\tilde{t}} + \frac{\partial\Pi_z}{\partial\tilde{t}}\frac{\partial\delta\Pi_z}{\partial\tilde{t}}\right)\mathrm{d}V, \tag{2.14}$$

Infusion of Eq. (2.4) in Eq. (2.14) results in the following:

$$\delta T = \int_0^L \left(\begin{array}{l} I_0^\star \left(\frac{\partial \Pi}{\partial \tilde{t}} \frac{\partial \delta \Pi}{\partial \tilde{t}} + \frac{\partial (w_\mathrm{b} + w_\mathrm{s})}{\partial \tilde{t}} \frac{\partial \delta (w_\mathrm{b} + w_\mathrm{s})}{\partial \tilde{t}} \right) \\ \quad - I_1^\star \left(\frac{\partial \Pi}{\partial \tilde{t}} \frac{\partial^2 \delta w_\mathrm{b}}{\partial x \partial \tilde{t}} + \frac{\partial^2 w_\mathrm{b}}{\partial x \partial \tilde{t}} \frac{\partial \delta \Pi}{\partial \tilde{t}} \right) \\ \quad - J_1^\star \left(\frac{\partial \Pi}{\partial \tilde{t}} \frac{\partial^2 \delta w_\mathrm{s}}{\partial x \partial \tilde{t}} + \frac{\partial^2 w_\mathrm{s}}{\partial x \partial \tilde{t}} \frac{\partial \delta \Pi}{\partial \tilde{t}} \right) \\ + I_2^\star \frac{\partial^2 w_\mathrm{b}}{\partial x \partial \tilde{t}} \frac{\partial^2 \delta w_\mathrm{b}}{\partial x \partial \tilde{t}} + K_2^\star \frac{\partial^2 w_\mathrm{s}}{\partial x \partial \tilde{t}} \frac{\partial^2 \delta w_\mathrm{s}}{\partial x \partial \tilde{t}} \\ + J_2^\star \left(\frac{\partial^2 w_\mathrm{b}}{\partial x \partial \tilde{t}} \frac{\partial^2 \delta w_\mathrm{s}}{\partial x \partial \tilde{t}} + \frac{\partial^2 w_\mathrm{s}}{\partial x \partial \tilde{t}} \frac{\partial^2 \delta w_\mathrm{b}}{\partial x \partial \tilde{t}} \right) \end{array} \right), \quad (2.15)$$

In accordance with the magnetic and temperature effect,

$$f_\mathrm{B} = \eta A \Omega_x^2 \frac{\partial^2 w}{\partial x^2} \quad N_T = \int_{-h/2}^{h/2} E(z) \lambda(z) \Delta T \mathrm{d}z,$$

where f_B, η, A, and Ω_x stand for the magnetic force, magnetic field permeability, cross sectional area of the nanobeam, and the magnetic potential of the longitudinal magnetic field. For an FG nanobeam, it is assumed that the temperature can be distributed uniformly across its thickness and the temperature gradient at stress free state is ΔT.

In the above definition, the inertia of mass moments can be defined as follows:

$$[I_0^\star, I_1^\star, I_2^\star, J_1^\star, J_2^\star, K_2^\star] = \int_A [1, z, z^2, f(z), zf(z), f^2(z)] \rho(z) \mathrm{d}A$$

and the work done N_x with a temperature gradient of thermal effect can be defined as follows:

$$\delta V = \left(\frac{1}{2} \int_0^l N_x + N_T \left(\frac{\partial w}{\partial x} \frac{\partial \delta w}{\partial x} \right) + \eta \Omega_x^2 \frac{\partial^2 w}{\partial x^2} \right) \mathrm{d}x, \quad (2.16)$$

By inserting the Eqs. (2.11) and (2.15) in Eq. (2.8), the equation of the beam in Euler–Lagrange can be derived and the outcome can be coupled as follows:

$$\frac{\partial N}{\partial x} = I_0^\star \frac{\partial^2 \Pi}{\partial \tilde{t}^2} - I_1^\star \frac{\partial^3 w_\mathrm{b}}{\partial x \partial \tilde{t}^2} - J_1^\star \frac{\partial^3 w_\mathrm{s}}{\partial x \partial \tilde{t}^2}, \quad (2.17)$$

$$\begin{aligned} \frac{\partial^2 M_\mathrm{b}}{\partial x^2} &= I_0^\star \frac{\partial^2 (w_\mathrm{b} + w_\mathrm{s})}{\partial \tilde{t}^2} + I_1^\star \frac{\partial^3 \Pi}{\partial x \partial \tilde{t}^2} - I_2^\star \frac{\partial^4 w_\mathrm{b}}{\partial x^2 \partial \tilde{t}^2} \\ &\quad - J_2^\star \frac{\partial^4 w_\mathrm{s}}{\partial x^2 \partial \tilde{t}^2} - \left(N_x + N_T \left(\frac{\partial^2 w}{\partial x^2} + \eta \Omega_x^2 \frac{\partial^2 w}{\partial x^2} \right) \right), \quad (2.18) \end{aligned}$$

$$\begin{aligned} &\frac{\partial^2 M_\mathrm{b}}{\partial x^2} + \frac{\partial Q}{\partial x} - N_x \frac{\partial^2 w}{\partial x^2} \\ &= \left(I_0^\star \frac{\partial^2 (w_\mathrm{b} + w_\mathrm{s})}{\partial \tilde{t}^2} + J_1^\star \frac{\partial^3 \Pi}{\partial x \partial \tilde{t}^2} - J_2^\star \frac{\partial^4 w_\mathrm{b}}{\partial x^2 \partial \tilde{t}^2} \right. \\ &\quad \left. - K_2^\star \frac{\partial^4 w_\mathrm{s}}{\partial x^2 \partial \tilde{t}^2} \right) - \left(N_x + N_T \left(\frac{\partial^2 w}{\partial x^2} + \eta \Omega_x^2 \frac{\partial^2 w}{\partial x^2} \right) \right), \quad (2.19) \end{aligned}$$

$$\delta \phi = \int_{\frac{-h}{2}}^{\frac{h}{2}} \left[\cos(\beta z) \left(\frac{\partial Dx}{\partial x} \right) \right] + \beta \sin(\beta z) Dz. \quad (2.20)$$

3 Nonlocal state-space model

This section demonstrates the nonlocality stress and strain effects on the time–space domains, when the wave length or excitation frequency interferes with time and intrinsic characteristic length. Nonlocal time–space viscoelasticity problems are based on the combination of the Boltzmann superposition integral and the Eringen concept of nonlocal elasticity. Accordingly, integral stress in nonlinear state and strain equations are stated as follows:

$$\begin{aligned} &\int_{-\infty}^{t} \int_{V} (K_\sigma(\tilde{t} - \tau, |r - r'|) \sigma_{ij}(r', \tau) \mathrm{d}r' \mathrm{d}\tau) \\ &= \int_{-\infty}^{t} \int_{V} K_\varepsilon(\tilde{t} - \tau, |r - r'|) C_{ijkl} \varepsilon_{kl}(r', \tau) \mathrm{d}r' \mathrm{d}\tau, \end{aligned} \quad (3.1)$$

where σ_{ij} and ε_{kl} are the stress and strain tensor arrays and the nonlocal kernel functions are $K_\sigma(\tilde{t} - \tau, |r - r'|)$ and $K_\varepsilon(\tilde{t} - \tau, |r - r'|)$. Eq. (3.1) can be read in the following form *via* Fourier, inverse Fourier, and Taylor series,

$$\left(1 - l_\sigma^2 \nabla^2 + \tau_\sigma \frac{\partial}{\partial \tilde{t}} \right) \sigma_{ij} = C_{ijkl} \left(1 - l_\varepsilon^2 \nabla^2 + \tau_\varepsilon \frac{\partial}{\partial \tilde{t}} \right) \varepsilon_{kl}, \quad (3.2)$$

To balance the absence of stiffness-hardening behavior, the nonlocal strain gradient elasticity must be incorporated in the equation. The following relation can be used to derive the nonlocal strain gradient viscoelasticity with fraction.

$$\left(1 - l_\sigma^2 \nabla^2 + \tau_\sigma \frac{\partial}{\partial \tilde{t}} \right) \sigma_{ij} = C_{ijkl} \left(1 - l_\varepsilon^2 \nabla^2 + \tau_\varepsilon \frac{\partial}{\partial \tilde{t}} \right) \varepsilon_{kl}, \quad (3.3)$$

The Kelvin–Voigt relation of viscoelastic material with three parameters in a solid state is given as follows:

$$(1-\mu^2\nabla^2)\sigma_{ij} = C_{ijkl}\left(1-\lambda^2\nabla^2+\tau\frac{\partial}{\partial\tilde{t}}\right)\varepsilon_{kl}, \tag{3.4}$$

where $\lambda = l_\varepsilon$ and $\mu = l_\sigma$ are length scale and nonlocal parameters, respectively. The relation between rheological character and spatial nonlocality of the system is designed as $\tau = \mu\sqrt{\frac{\tau_c}{E_c}}$. From Eqs. (2.12) and (2.13), the displacement field having resultant stress over the area of cross section of the beam can be computed as follows:

$$\begin{aligned}(1-\mu^2\nabla^2)N = &\left(1-\lambda^2\nabla^2+\tau\frac{\partial}{\partial\tilde{t}}\right)\\ &\times\left(A_{xx}\frac{\partial u}{\partial x}-B_{xx}\frac{\partial^2 w_b}{\partial x^2}-B^s_{xx}\frac{\partial^2 w_s}{\partial x^2}\right)\\ &-e_{31}E_z,\end{aligned} \tag{3.5}$$

$$\begin{aligned}(1-\mu^2\nabla^2)M^b = &\left(1-\lambda^2\nabla^2+\tau\frac{\partial}{\partial\tilde{t}}\right)\\ &\times\left(B_{xx}\frac{\partial u}{\partial x}-D_{xx}\frac{\partial^2 w_b}{\partial x^2}-D^s_{xx}\frac{\partial^2 w_s}{\partial x^2}\right)\\ &-(N_x+N_T-\eta\Omega_x^2)\frac{\partial^2 w}{\partial x^2}-e_{31}E_z,\end{aligned} \tag{3.6}$$

$$\begin{aligned}(1-\mu^2\nabla^2)M^s = &\left(1-\lambda^2\nabla^2+\tau\frac{\partial}{\partial\tilde{t}}\right)\\ &\times\left(B^s_{xx}\frac{\partial u}{\partial x}-D^s_{xx}\frac{\partial^2 w_b}{\partial x^2}-H^s_{xx}\frac{\partial^2 w_s}{\partial x^2}\right)\\ &-(N_x+N_T-\eta\Omega_x^2)\frac{\partial^2 w}{\partial x^2}-e_{31}E_z,\end{aligned} \tag{3.7}$$

$$\begin{aligned}(1-\mu^2\nabla^2)Q^{xz} = &\left(1-\lambda^2\nabla^2+\tau\frac{\partial}{\partial\tilde{t}}\right)\times\left(A^s_{xx}\frac{\partial w_s}{\partial x}\right)\\ &-(N_x+N_T-\eta\Omega_x^2)\frac{\partial^2 w}{\partial x^2}-e_{15}E_x,\end{aligned} \tag{3.8}$$

$$(1-\mu^2\nabla^2)D_x = e_{15}\gamma_{xz}+e_{11}E_x, \tag{3.9}$$

$$(1-\mu^2\nabla^2)D_z = e_{31}\varepsilon_{xx}+e_{33}E_z, \tag{3.10}$$

where cross sectional rigidities are

$$\begin{aligned}&[A_{xx}, B_{xx}, B^s_{xx}, D_{xx}, D^s_{xx}, H^s_{xx}]\\ &= \int_A [1, z, f(z), z^2, zf(z), f^2(z)],\end{aligned} \tag{3.11}$$

$$A^s = \int_A g^2(z)G(z)\mathrm{d}A, \tag{3.12}$$

where $e_{31}E_x = e_{31}(\cos(\beta z))\frac{\partial\phi}{\partial x}$ and $e_{15}E_z = e_{15}\left(-\beta\sin(\beta z)\phi-\frac{2V_0 e^{ikt}}{h}\right)$.

4 Governing equations

Eqs. (3.5)–(3.10) must be substituted in equations (2.17)–(2.20). Now the governing equations are as follows:

$$\begin{aligned}&\left(1-\lambda^2\nabla^2+\tau\frac{\partial}{\partial\tilde{t}}\right)\left(A_{xx}\frac{\partial^2\Pi}{\partial x^2}-B_{xx}\frac{\partial^3 w_b}{\partial x^3}-B^s_{xx}\frac{\partial^3 w_s}{\partial x^3}\right)\\ &+(1-\mu^2\nabla^2)\left(-I_0\ddot{\Pi}+I_1\frac{\partial\ddot{w}_b}{\partial x}+J_1\frac{\partial\ddot{w}_s}{\partial x}\right)\\ &-\left(N_x+N_T-\eta\Omega_x^2\left(\frac{\partial^2 w}{\partial x^2}\right)\right)-e_{31}E_z=0,\end{aligned} \tag{4.1}$$

$$\begin{aligned}&\left(1-\lambda^2\nabla^2+\tau\frac{\partial}{\partial\tilde{t}}\right)\left(B_{xx}\frac{\partial^3\Pi}{\partial x^3}-D_{xx}\frac{\partial^4 w_b}{\partial x^4}-D^s_{xx}\frac{\partial^4 w_s}{\partial x^4}\right)\\ &+(1-\mu^2\nabla^2)\left(-I_0(\ddot{w}_b+\ddot{w}_s)-I_1\frac{\partial\ddot{\Pi}}{\partial x}+I_2\frac{\partial^2\ddot{w}_b}{\partial x^2}\right.\\ &\left.+J_2\frac{\partial^2\ddot{w}_s}{\partial x^2}\right)-\left(N_x+N_T-\eta\Omega_x^2\left(\frac{\partial^2 w}{\partial x^2}\right)\right)-e_{31}E_z=0,\end{aligned} \tag{4.2}$$

$$\begin{aligned}&\left(1-\lambda^2\nabla^2+\tau\frac{\partial}{\partial\tilde{t}}\right)\left(B^s_{xx}\frac{\partial^3\Pi}{\partial x^3}-D^s_{xx}\frac{\partial^4 w_b}{\partial x^4}\right.\\ &\left.-H^s_{xx}\frac{\partial^4 w_s}{\partial x^4}+A^s\frac{\partial^2 w_s}{\partial x^2}\right)+(1-\mu^2\nabla^2)\left(-I_0(\ddot{w}_b+\ddot{w}_s)\right.\\ &\left.-J_1\frac{\partial\ddot{\Pi}}{\partial x}+J_2\frac{\partial^2\ddot{w}_b}{\partial x^2}+K_2\frac{\partial^2\ddot{w}_s}{\partial x^2}\right)\\ &-\left(N_x+N_T-\eta\Omega_x^2\left(\frac{\partial^2 w}{\partial x^2}\right)\right)-e_{31}E_z-e_{15}E_x=0.\end{aligned} \tag{4.3}$$

5 Analytical solution

The governing equation obtained in Section 4 will be solved in this section. The analytical wave dispersion method is used in this case to solve the problems of wave propagation for various types of structures, including beams, plates, and shells. A higher order beam's solution function can be in the form as follows:

$$\begin{Bmatrix}\Pi\\ w_b\\ w_s\end{Bmatrix} = \begin{Bmatrix}\Pi\exp[i(\beta x-\omega\tilde{t})]\\ w_b\exp[i(\beta x-\omega\tilde{t})]\\ w_s\exp[i(\beta x-\omega\tilde{t})]\end{Bmatrix}, \tag{5.1}$$

where Π, w_b, and w_s are the anonymous amplitudes of propagating waves. Here ω & β are frequency and wave number, respectively. By substituting the above expression in Eqs. (4.1)–(4.3), the achieved form will be as follows:

$$\{[K] + [C]\omega + [M]\omega^2\}\begin{Bmatrix} \Pi \\ w_b \\ w_s \end{Bmatrix} = 0, \tag{5.2}$$

where damping and mass matrices are given by $[K]$, $[C]$, and $[M]$ respectively. The components of these symmetric matrices are as follows:

$$\begin{aligned}
k_{11} &= (1 + \lambda^2\beta^2)A_{xx}\beta^2 \\
k_{12} &= i(N_x + \eta\Omega_x^2)(1 + \lambda^2\beta^2)B_{xx}\beta^5 \\
k_{13} &= i(N_x + \eta\Omega_x^2)(1 + \lambda^2\beta^2)B_{xx}^s\beta^5 \\
k_{14} &= e_{31}(1 - \lambda^2\beta^2)\beta\ \sin(\beta z)\phi - \frac{2V_0 e^{ikt}}{h} \\
k_{22} &= -(N_x + \eta\Omega_x^2)N_T(1 + \lambda^2\beta^2)D_{xx}\beta^6 \\
k_{23} &= -(N_x + \eta\Omega_x^2)N_T(1 + \lambda^2\beta^2)D_{xx}^s\beta^6 \\
k_{24} &= e_{31}(1 - \lambda^2\beta^2)\beta\ \sin(\beta z)\phi - \frac{2V_0 e^{ikt}}{h} \\
k_{33} &= -(N_x + \eta\Omega_x^2)N_T(1 + \lambda^2\beta^2)(H_{xx}^s\beta^6 + A^s\beta^4) \\
k_{34} &= e_{31}(1 - \lambda^2\beta^2)\beta^2\ \sin(\beta z)\phi - \frac{2V_0 e^{ikt}}{h},
\end{aligned} \tag{5.3}$$

$$\begin{aligned}
c_{11} &= -A_{xx}\tau\beta^2 \\
c_{12} &= i(N_x + \eta\Omega_x^2)B_{xx}\tau\beta^5 \\
c_{13} &= i(N_x + \eta\Omega_x^2)B_{xx}^s\tau\beta^5 \\
c_{22} &= -(N_x + \eta\Omega_x^2)D_{xx}\tau\beta^6 \\
c_{23} &= -(N_x + \eta\Omega_x^2)D_{xx}^s\tau\beta^6 \\
c_{24} &= \tau e_{31}\left(\beta^2\ \cos(\beta z)\frac{\mathrm{d}z}{\mathrm{d}t}\phi - \left(\frac{2V_0 e^{ikt}}{h}(ik)\right)\right) \\
c_{33} &= -(N_x + \eta\Omega_x^2)\tau\beta^4(H_{xx}^s\beta^2 + A_s) \\
c_{34} &= \tau e_{31}\left(\beta^2\ \cos(\beta z)\frac{\mathrm{d}z}{\mathrm{d}t}\phi - \left(\frac{2V_0 e^{ikt}}{h}(ik)\right)\right),
\end{aligned} \tag{5.4}$$

$$\begin{aligned}
m_{11} &= -(1 + \mu^2\beta^2)I_0^\star \\
m_{12} &= i(N_x + \eta\Omega_x^2)\beta^2(1 + \mu^2\beta^2)I_1^\star \\
m_{13} &= i(N_x + \eta\Omega_x^2)\beta^2(1 + \mu^2\beta^2)J_1^\star \\
m_{22} &= -(1 + \mu^2\beta^2)(I_0^\star + I_2^\star(N_x + \eta\Omega_x^2)\beta^4) \\
m_{23} &= -(1 + \mu^2\beta^2)(I_0^\star + J_2^\star(N_x + \eta\Omega_x^2)\beta^4) \\
m_{33} &= -(1 + \mu^2\beta^2)(I_0^\star + K_2^\star(N_x + \eta\Omega_x^2)\beta^2) \\
m_{34} &= (1 + \mu^2\beta^2)e_{31}\left(\beta^2\ \cos(\beta z)\frac{\mathrm{d}z}{\mathrm{d}t}\phi \right. \\
&\quad \left. - \left(\frac{2V_0 e^{ikt}}{h}(ik)\right)\right).
\end{aligned} \tag{5.5}$$

6 Results and discussion

This section illustrates the magneto-thermo vibration of FG nanobeam with the numerical examples. The material properties are composed of $BaTiO_3$ and $CoFe_2O_4$, which are presented in Table 1. Table 2 shows the comparison of the buckling load for various power-law exponent values. Whereas, Table 3 gives the variation in the magnetic potential and electric voltages with the varying and increasing nonlocal parameter. Since an increasing nonlocal parameter shows a decrement with the magnetic potential (Ω) and the electric voltage (V).

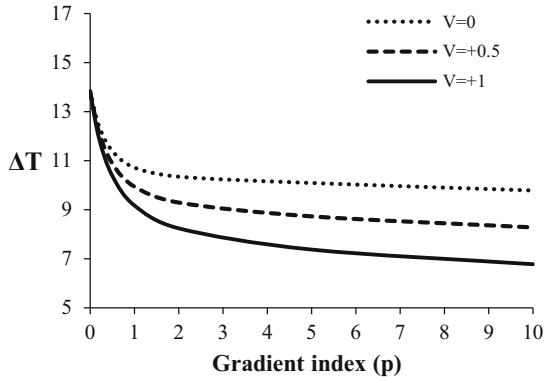

Figure 2: External voltage with the presence of rising temperature to gradient index for $\mu = 1.0$.

Now, Figures 2 and 3 highlight the effect of external voltage (V) with the variation in the rising temperature (ΔT) and the gradient index (p) for $\mu = 1.0$ & 1.5. Whereas, with the increase in the external voltage ($V = 0$, 0.5, and 1), the temperature gradually decreases with respect to the gradient index (p) and nonlocal parameter. Figure 4 shows the decrement in the buckling load with an increase in the magnetic effect (Ω) and the nonlocal value (μ). Also, when there is no magnetic effect found, the buckling load at some point decreases with the increse in the value of the nonlocal (μ). Figure 5 presents the variation in the dimensionless buckling load with the nonlocal parameter (μ) in the effect of the external voltage (V). Since there is an increase in the voltage (V), the dimensionless buckling load declines and gets neutralized at some point of the nonlocal parameter. Figures 6 and 7 depict the effect of gradient index with respect to

Table 1: MEE coefficients of material properties

Material	Properties			
$BaTiO_3$	E (Pa)	166	e_{33} (N/m^2 K)	(7.124×10^{-9})
	ρ (kg/m^3)	5,800	e_{15} (c/m^2)	14.1
	v (–)	1.1945		
$CoFe_2O_4$	E (Pa)	286	e_{31} (c/m^2)	–(4.1)
	ρ (kg/m^3)	5,300	e_{11} (c/V m)	(5.841×10^{-9})
	v (–)	1.167		

Table 2: Comparison of FGM beam non-dimensional buckling for various power-law exponents

L/h		$p = 0$	$p = 0.5$	$p = 1$	$p = 2$	$p = 5$	$p = 10$
5	Nguyen *et al.* (2015)	48.8406	32.0013	24.6894	19.1577	15.7355	14.1448
	Present	48.835	31.967	24.6870	19.1605	15.7401	14.13
10	Nguyen *et al.* (2015)	52.3083	34.0002	26.1707	20.3909	17.1091	15.5278
	Present	52.3082	34.0087	26.1727	20.3936	17.1118	15.5291

Table 3: Dimensionless frequency of an FG nanobeam varies with nonlocal parameters, electric voltages, and magnetic potentials

μ		$p = 0.2$			$p = 1$			$p = 5$		
		$V = -5$	$V = 0$	$V = +5$	$V = -5$	$V = 0$	$V = +5$	$V = -5$	$V = 0$	$V = +5$
0	$\Omega = -0.05$	8.34927	7.68726	7.24086	8.3637	7.69636	7.24398	8.3781	7.70545	7.24711
	$\Omega = 0$	8.34708	7.68034	7.22898	8.36151	7.68946	7.23212	8.37592	7.69856	7.23525
	$\Omega = -0.05$	8.34489	7.67343	7.21709	8.35933	7.68255	7.22023	8.37373	7.69166	7.22337
1	$\Omega = -0.05$	7.96429	7.33365	6.9088	7.97941	7.34319	6.91208	7.9945	7.35273	6.91536
	$\Omega = 0$	7.96199	7.32641	6.89636	7.97712	7.33596	6.89964	7.99222	7.3455	6.90293
	$\Omega = -0.05$	7.95969	7.31915	6.88389	7.97483	7.32872	6.88718	7.98993	7.33827	6.89047
2	$\Omega = -0.05$	7.62789	7.02471	6.61874	7.64368	7.03468	6.62216	7.65944	7.04462	6.62558
	$\Omega = 0$	7.6255	7.01715	6.60575	7.64129	7.02712	6.60917	7.65705	7.03708	6.6126
	$\Omega = -0.05$	7.6231	7.00958	6.59273	7.6389	7.01956	6.59617	7.65466	7.02953	6.5996
3	$\Omega = -0.05$	7.33065	6.75176	6.3625	7.34708	6.76213	6.36606	7.36347	6.77248	6.36962
	$\Omega = 0$	7.32816	6.74389	6.34898	7.34459	6.75427	6.35255	7.36099	6.76463	6.35612
	$\Omega = -0.05$	7.32566	6.73601	6.33544	7.3421	6.7464	6.33902	7.3585	6.75678	6.34259
0	$\Omega = -0.05$	8.55703	8.31260	8.37748	9.43205	8.84645	8.55259	10.2325	9.34987	8.72418
	$\Omega = 0$	8.41640	7.88376	7.67745	9.30465	8.44476	7.86815	10.1152	8.97075	8.05433
	$\Omega = -0.05$	8.27337	7.43021	6.90683	9.17548	8.02299	7.11820	9.99651	8.57489	7.32348
1	$\Omega = -0.05$	8.08984	7.91790	8.03872	9.01035	8.47664	8.22104	9.84516	9.00077	8.39941
	$\Omega = 0$	7.94094	7.46642	7.30630	8.87690	8.05654	7.50644	9.72317	8.60629	7.70137
	$\Omega = -0.05$	7.78919	6.98583	6.49177	8.74141	7.61329	6.71622	9.59964	8.19284	6.93341
2	$\Omega = -0.05$	7.67792	7.57252	7.74446	8.64241	8.15496	7.93354	9.50958	8.69849	8.11823
	$\Omega = 0$	7.52087	7.09911	6.98123	8.50319	7.71737	7.19042	9.38323	8.28964	7.39369
	$\Omega = -0.05$	7.36046	6.59180	6.12362	8.36165	7.25342	6.36107	9.25516	7.85955	6.58997
3	$\Omega = -0.05$	7.31058	7.26690	7.48595	8.31777	7.87198	7.68141	9.21554	8.43377	7.87201
	$\Omega = 0$	7.14545	6.77216	6.69332	8.17302	7.41771	6.91123	9.08510	8.01142	7.12247
	$\Omega = -0.05$	6.97642	6.23831	5.79324	8.02566	6.93375	6.04369	8.95277	7.56553	6.28416

the presence of the dimensionless buckling load and magnetic potential for different nonlocal values. Therefore, with the surge effect of the gradient index (p), there is an increase in the magnetic potential with the decrease in the dimensionless bucklingload and ampilifies over the nonlocal parameter (μ). Figures 8 and 9 represent the impact of the electric voltage and dimensionless buckling load in the presence of the gradient index $p = 0$, 1, 5 over nonlocal parameter (μ). Hence, when the gradient index is null, there is no fluctuation in the buckling load and forms a linear effect and nonlocal values ampilify the buckling load. So, if the gradient index rises, then the electric voltage increases with the decrease in buckling load gradually. Figures 10 and 11 interpret that temperature (ΔT) stabilizes with an increase in the gradient index and magnetic potential. Thus, when the magnetic potential $\Omega = 0$,

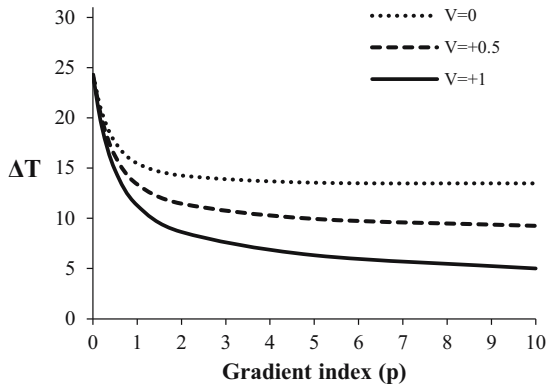

Figure 3: External voltage in the presence of temperature with respect to gradient index for μ = 1.5.

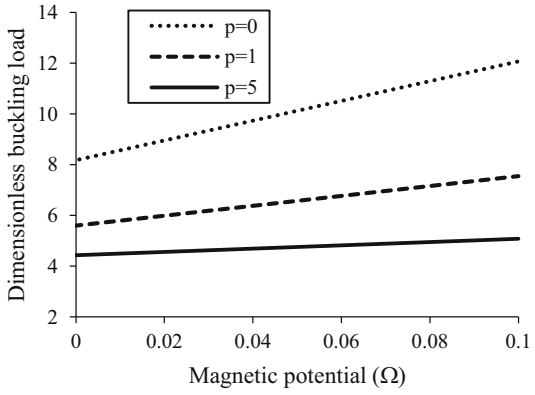

Figure 6: Gradient index with the presence of rising dimensionless buckling load to magnetic potential for μ = 1.0.

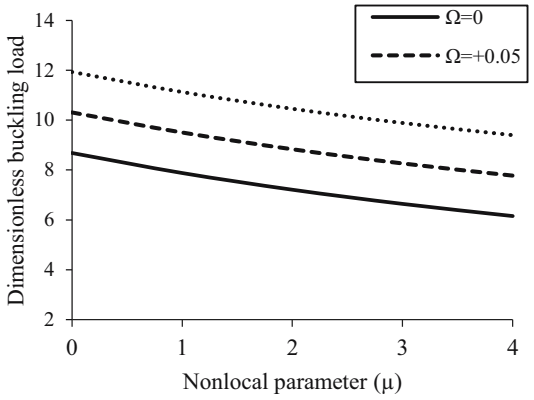

Figure 4: Magnetic potential on the dimensionless buckling with respect to nonlocal parameter.

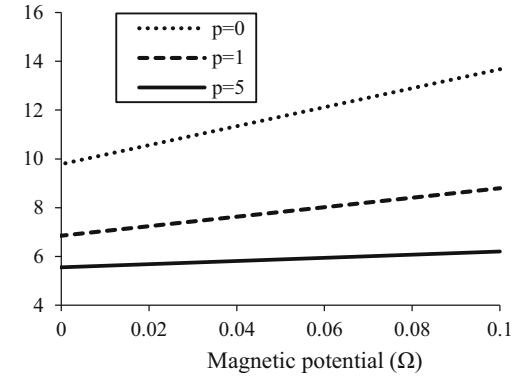

Figure 7: Gradient index in the presence of dimensionless buckling load to magnetic potential μ = 1.5.

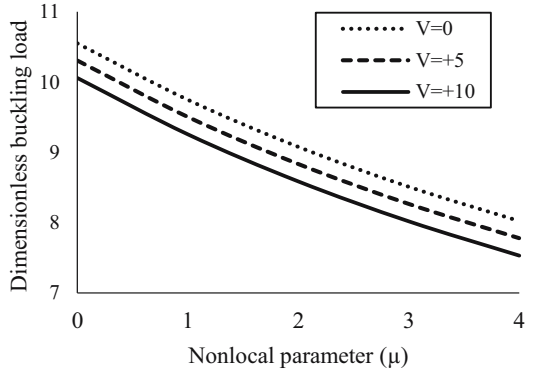

Figure 5: External voltage on the dimensionless buckling load with respect to nonlocal parameter.

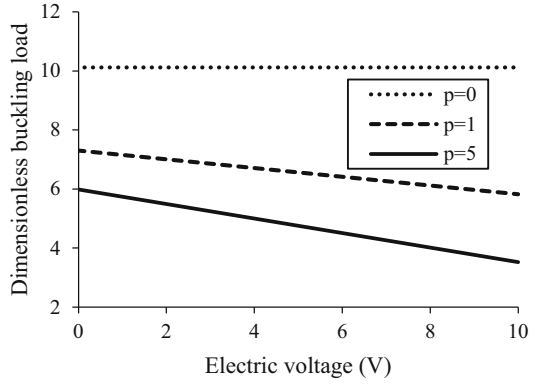

Figure 8: Gradient index in the presence of dimensionless buckling load to electric voltage when μ = 1.0.

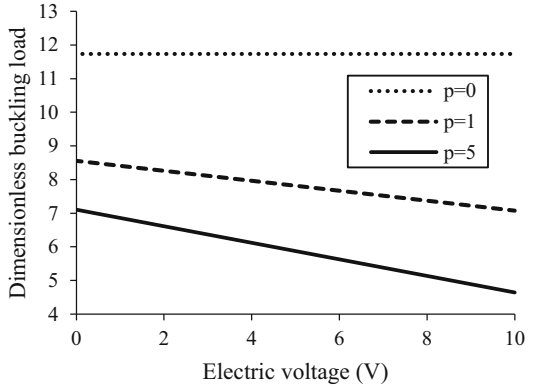

Figure 9: Gradient index in the presence of dimensionless buckling load to electric voltage when μ = 1.5.

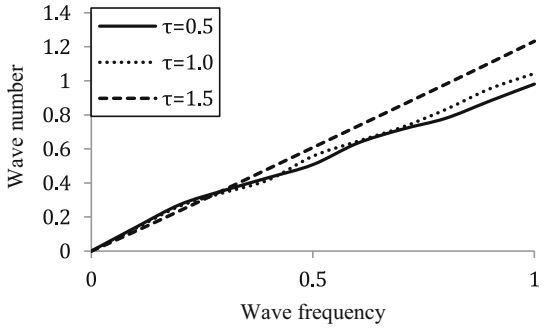

Figure 12: Damping factor in the presence of wave number with respect to wave frequency for μ = 1.0.

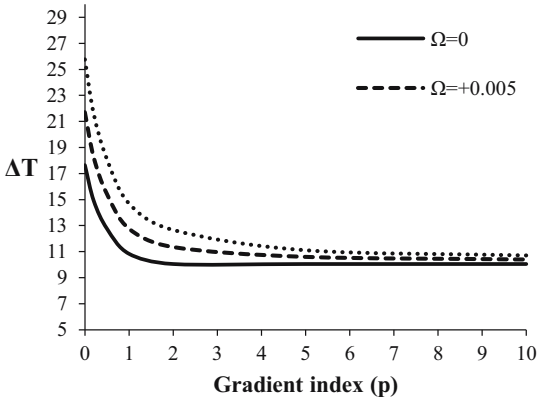

Figure 10: Magnetic potential in the presence of temperature with respect to gradient index for μ = 1.0.

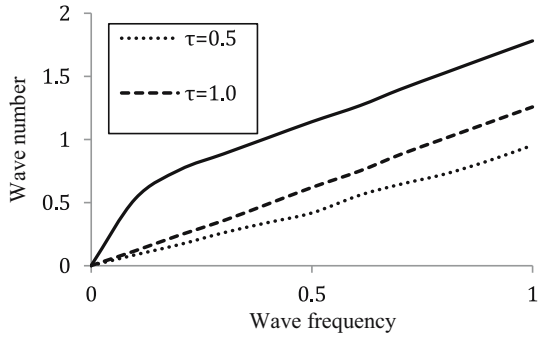

Figure 13: Damping factor in the presence of wave number with respect to wave frequency for μ = 1.5.

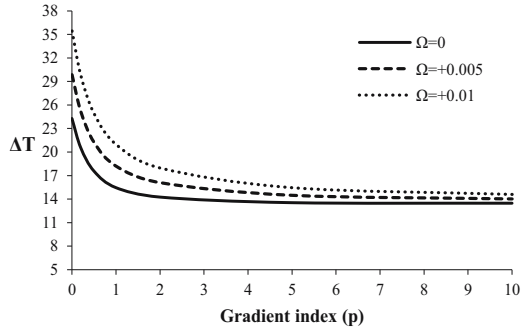

Figure 11: Magnetic potential in the presence of temperature with respect to gradient index for μ = 1.5.

the temperature calms down and stabilizes at some point with respect to an increase in the gradient index (p) and nonlocal values. Figures 12 and 13 show the effect of an internal damping factor (τ) in the existence of wave number and wave frequency over nonlocal parameter (μ).

In these figures, the damping factor with $\tau \geq 1.5$ shows a raising linear value and when $\tau \leq 0.5$, there is an oscillation in the wave number and wave frequency.

7 Conclusion

The above study shows the wave propagation analysis of piezoelectric FGM nanobeam. Magneto thermo properties of the FG nanobeam are considered to be the function of thickness according to the power-law model. The governing equations are extracted by substituting the structure displacement field equations in the beam's Euler–Lagrange equations and are framed as symmetric matrices components to arrive at required solutions. Hence, the upshots of the work are as follows:

- The stability behaviors of FGM nanobeam are affected .by magneto thermo piezo electricity and nonlocal values.

- Physical variants could be controlled *via* applying a suitable value of damping factor.
- Natural frequency reduces, while the nonlocal parameter and gradient index of the FG nanobeam amplify.
- The increase in power-law index softens the volume fraction.
- The bending rigidity and phase velocities are high in amplified wave numbers and get reversed in low wave numbers.

Acknowledgments: The authors would like to thank the reviewers for their useful comments and appropriate revisions of the manuscript.

Funding information: The authors state no funding involved.

Author contributions: All authors have accepted responsibility for the entire content of this manuscript and approved its submission.

Conflict of interest: Rossana Dimitri and Francesco Tornabene, who are the co-authors of this article, are current Editorial Board members of *Curved and Layered Structures*. This fact did not affect the peer-review process. The authors declare no other conflict of interest.

Data availability statement: The datasets analysed during the current study are available from the corresponding author on reasonable request.

References

[1] Ke LL, Wang YS, Wang ZD. Nonlinear vibration of piezoelectric based on the nonlocal theory. Compos Struct. 2012;94:2038–47.
[2] Ke LL, Wang YS. Thermoelectric-mechanical vibration of piezoelectric nanobeams based on the nonlocal theory. Smart Mater Struct. 2012;21:025018.
[3] Ebrahimi F. Wave dispersion in viscoelastic FG nanobeam *via* a novel spatial – temporal nonlocal strain gradient framework. Waves Random Complex Media. 2021. https://doi.org/10.1080/17455030.2021.1970282.
[4] Ebrahimi F, Barati MR. Vibration analysis of smart piezoelectrically actuated nanobeams subjected to magneto-electrical field in thermal environment. J Vib Control. 2018;24:549–64.
[5] Zaoui FZ, Ouinas D, Tounsi A. New 2D and quasi-3D shear deformation theories for free vibration of functionally graded plates on elastic foundations. Compos B: Eng. 2019;159:231–47.
[6] Alibeigi B, Tadi Beni Y, Mehralian F. On the thermal buckling of magneto-electro-elastic piezoelectric nanobeams. Eur Phys J Plus. 2018;133:133.
[7] Shariati A, Ebrahimi F, Karimiasl M, Selvamani R, Toghroli A. On bending characteristics of smart magneto-electro-piezoelectric nanobeams system. Adv Nano Res. 2020;9:183–91.
[8] Ebrahimi F, Karimiasl M, Selvamani R. Bending analysis of magneto-electro piezoelectric nanobeams system under hygro-thermal loading. Adv Nano Res. 2020;8:203–14.
[9] Ebrahimi F, Dabbagh A. Wave propagation analysis of smart nanostructures. 1st ed. Boca Raton (FL): CRC Press; 2020.
[10] Li SR, Su HD, Cheng CJ. Free vibration of functionally graded material beams with surface-bonded piezoelectric layers in thermal environment. Appl Math Mech. 2019;30:969–82.
[11] Romano G, Barretta R. Stress-driven versus strain-driven nonlocal integral model for elastic nano-beams. Compos B: Eng. 2017;114:184–8.
[12] Barretta R, Fabbrocino F, Luciano R, de Sciarra FM. Closed-form solutions in stress-driven two-phase integral elasticity for bending of functionally graded nano-beams. Physica E Low Dimens Syst Nanostruct. 2018;97:13–30.
[13] Kiani Y, Eslami MR. Thermal buckling analysis of functionally graded material beams. Int J Mech Mater Des. 2010; 6:229–38.
[14] Sun D, Luo SN. Wave propagation of functionally graded material plates in thermal environments. Ultrasonics. 2011;51:940–52.
[15] Thai HT, Choi DH. A refined shear deformation theory for free vibration of functionally graded plates on elastic foundation. Compos B: Eng. 2012;43:2335–47.
[16] Thai HT, Park T, Choi DH. An efficient shear deformation theory for vibration of functionally graded plates. Arch Appl Mech. 2013;83:137–49.
[17] Shahsavari D, Shahsavari M, Li L, Karami B. A novel quasi-3D hyperbolic theory for free vibration of FG plates with porosities resting on Winkler/Pasternak/Kerr foundation. Aerosp Sci Technol. 2018;72:134–49.
[18] Eringen AC. On differential equations of nonlocal elasticity and solutions of screw dislocation and surface waves. J Appl Phys. 1983;54:4703–10.
[19] Civalek Ö, Demir Ç. Bending analysis of microtubules using nonlocal Euler–Bernoulli beam theory. Appl Math Model. 2011;35:2053–67.
[20] Arani AG, Amir S, Shajari AR, Mozdianfard MR. Electro-thermo-mechanical buckling of DWBNNTs embedded in bundle of CNTs using nonlocal piezoelasticity cylindrical shell theory. Compos B: Eng. 2012;43:195–203.
[21] Reddy JN, El-Borgi S. Eringen's nonlocal theories of beams accounting for moderate rotations. Int J Eng Sci. 2014;82:159–77.
[22] Zhang LL, Liu JX, Fang XQ, Nie GQ. Effects of surface piezoelectricity and nonlocal scale on wave propagation in piezoelectric nanoplates. Eur J Mech A Solids. 2014;46:22–9.
[23] Nejad MZ, Hadi A. Eringen's non-local elasticity theory for bending analysis of bi-directional functionally graded Euler–Bernoulli nano-beams. Int J Eng Sci. 2016;106:1–9.
[24] Nejad MZ, Hadi A. Non-local analysis of free vibration of bi-directional functionally graded Euler–Bernoulli nano-beams. Int J Eng Sci. 2016;105:1–11.
[25] Nejad MZ, Hadi A, Rastgoo A. Buckling analysis of arbitrary two-directional functionally graded Euler–Bernoulli nano-beams based on nonlocal elasticity theory. Int J Eng Sci. 2016;103:1–10.
[26] Ebrahimi F, Barati MR. Size-dependent vibration analysis of viscoelastic nanocrystalline silicon nanobeams with porosities

based on a higher order refined beam theory. Compos Struct. 2017;166:256–67.
[27] Lim CW, Zhang G, Reddy JN. A higher-order nonlocal elasticity and strain gradient theory and its applications in wave propagation. J Mech Phys Solids. 2015;78:298–313.
[28] Farajpour A, Haeri Yazdi MR, Rastgoo A, Mohammadi M. A higher-order nonlocal strain gradient plate model for buckling of orthotropic nanoplates in thermal environment. Acta Mech. 2016;227:1849–67.
[29] Li L, Li X, Hu Y. Free vibration analysis of nonlocal strain gradient beams made of functionally graded material. Int J Eng Sci. 2016;102:77–92.
[30] Ebrahimi F, Dabbagh A. Wave propagation analysis of embedded nanoplates based on a nonlocal strain gradient-based surface piezoelectricity theory. Eur Phys J Plus. 2017;132:449.
[31] Hadi A, Zamani Nejad M, Hosseini M. Vibrations of three-dimensionally graded nanobeams. Int J Eng Sci. 2018;128:12–23.
[32] Alibeigi B, Tadi Beni Y, Mehralian F. On the thermal buckling of magneto-electro-elastic piezoelectric nanobeams. Eur Phys J Plus. 2018;133:1–18.
[33] Ke LL, Wang YS. Free vibration of size-dependent magneto-electro-elastic nanobeams based on the nonlocal theory. Physica E: Low Dimens Syst Nanostruct. 2014;63:52–61.
[34] Ebrahimi F, Karimiasl M, Singhal A. Magneto-electro-elastic analysis of piezoelectric–flexoelectric nanobeams rested on silica aerogel foundation. Eng Comput. 2021;37:1007–14.
[35] Ebrahimi F, Karimiasl M, Selvamani R. Bending analysis of magneto-electro piezoelectric nanobeams system under hygro-thermal loading. Adv Nano Res. 2020;8:203–14.
[36] Ramezani SR, Mojra A. Stability analysis of conveying-nanofluid CNT under magnetic field based on nonlocal couple stress theory and fluid-structure interaction. Mech Based Des Struct Mach. 2020;51:583–600.
[37] Ebrahimi F, Barati MR. Vibration analysis of smart piezoelectrically actuated nanobeams subjected to magneto-electrical field in thermal environment. J Vib Control. 2018;24:549–64.
[38] Ebrahimi F, Barati MR, Dabbagh A. A nonlocal strain gradient theory for wave propagation analysis in temperature-dependent inhomogeneous nanoplates. Int J Eng Sci. 2016;107:169–82.
[39] Ebrahimi F, Salari E. Effect of various thermal loadings on buckling and vibrational characteristics of nonlocal temperature-dependent functionally graded nanobeams. Mech Adv Mater Struct. 2016;23:1379–97.
[40] Ebrahimi F, Barati MR. Hygrothermal effects on vibration characteristics of viscoelastic FG nanobeams based on nonlocal strain gradient theory. Compos Struct. 2017;159:433–44.
[41] Ebrahimi F, Salari E. Thermal buckling and free vibration analysis of size dependent Timoshenko FG nanobeams in thermal environments. Compos Struct. 2015;128:363–80.
[42] Ebrahimi F, Daman M. Nonlocal thermo-electro mechanical vibration analysis of smart curved FG piezoelectric Timoshenko nanobeam. Smart Struct Syst. 2017;20(3):351–68.
[43] Vo TP, Thai HT, Nguyen TK, Inam F, Lee J. A quasi-3D theory for vibration and buckling of functionally graded sandwich beams. Compos Struct. 2015;119:1–12.
[44] Jalaei MH, Arani AG, Nguyen-Xuan H. Investigation of thermal and magnetic field effects on the dynamic instability of FG Timoshenko nanobeam employing nonlocal strain gradient theory. Int J Mech Sci. 2019;161–162:105043.
[45] Karami B, Shahsavari D, Karami M, Li L. Hygrothermal wave characteristic of nanobeam-type inhomogeneous materials with porosity under magnetic field. Proc Inst Mech Eng C: J Mech Eng Sci. 2019;233(6):2149–69.